COBEM 2021 26th International Congress of Mechanical Engineering
November 22-26, 2021, Virtual Congress, Brazil

COB-2021-0210
MULTI-BLOCK LATTICE BOLTZMANN METHOD APPLIED TO CONDUCTION IN TWO SOLIDS WITH LARGE DIFFERENCE BETWEEN THERMAL DIFFUSIVITIES

Ivan Talão Martins
Luben Cabezas Gómez
São Carlos School of Engineering - University of São Paulo
ivanmartins@usp.br and lubencg@sc.usp.br

Abstract. *Many real conjugate heat transfer problems involve materials with high differences between their thermal properties. Treating them with the conventional Lattice Boltzmann method (LBM) becomes a challenge, because there are problems involving the simulation scales which impact in the relaxation times (τ) values for both materials. Appropriate values in fluid region lead to not appropriate values in solid region, decreasing the results accuracy. This is addressed with the conventional multi-block (MB) scheme in LBM. In the paper it is proposed an improvement of the conventional MB scheme, that allows a free choose of relaxation time, not used in the conventional MB-LBM. Thereby, it is first studied a 2D conduction problem to verify the improved MB-LBM. Secondly, two 2D conduction problems are solved considering low and high differences between the thermal diffusivity of the materials, respectively. Both problems are solved with the conventional LBM, LB-LBM and the improved MB-LBM, concluding that the improved MB-LBM allows to study conjugate heat transfer problems involving large difference between the materials thermal properties, improving the accuracy and stability of the method.*

Keywords: *Lattice Boltzmann method, conjugate heat transfer problem, multi-block, heat diffusion problem.*

1. Introduction

Refrigeration and heating systems adopt in a large scale the use of heat exchangers with channels, and more recently, with microchannels. An important aspect in these system is related to the maximization of heat transfer, or just its increase in a satisfactory balance between cost and efficiency. Hence, it is necessary to know the behavior of these devices, being by the use of appropriate correlations or by numerical simulations. This work focuses on the improvement of one numerical simulation method for this purpose: the Lattice Boltzmann Method (LBM).

The LBM is a numerical mesoscopic method which was born in the 20st century, after the development of the Lattice Gas Automaton Wolf-Gladrow (2004). Currently, many variations of the method are presented in the open literature Guo and Shu (2013); Krüger *et al.* (2017); Mohamad (2019). One of these variations is the Multi-block LBM (MB-LBM). This method consists in the LBM application with non-uniform discretization of the lattices. In other words, the domain can be divided in regions, each one with a different lattice size. The MB-LBM represents a flexibilization of the conventional LBM, which only allows the use of uniform lattices Guo and Shu (2013).

The conventional LBM is extensively used in the simulation of fluid flow and heat transfer problems. In fact, the works by Aursjø *et al.* (2017), Pirouz *et al.* (2011) and Wang *et al.* (2007) make use of LBM to study the conjugate heat transfer in channels with or without other geometries in their interior, such as obstacles or fins. The MB-LBM proposed and used in this work is an extension of MB-LBM found in literature, see Guo and Shu (2013).

The main aim of the present developments is the simulation of heat transfer problems between different materials with high differences between their thermal diffusivities. Problems involving just conduction or conduction and convection are addressed. Overall, it is proposed in this work an improvement of the MB-LBM, which gives more freedom and accuracy for the simulation of heat transfer problems found in real applications.

2. Theoretical Background

The LBM is based in the discretization of Boltzmann transport equation, both in time, space and velocity directions Mohamad (2019). This equation is given by Eq. (1), in which f is the density distribution function, c_d the component of the velocity vector in d direction, $\frac{F_d}{\rho}$ the specific body force and $\Omega(f)$, the collision operator, which represents the effect of the particles collision.

$$\frac{\partial f}{\partial t} + c_d \cdot \frac{\partial f}{\partial x_d} + \frac{F_d}{\rho} \cdot \frac{\partial f}{\partial c_d} = \Omega(f) \tag{1}$$

Despite of being principally used to deal with fluid flow, the LBM can also be used to simulate heat diffusion in solids and liquids (Ho *et al.*, 2002). Then, as f is commonly used to deal with flows, it is convenient to change f by g in Eq. (1), just in order to follow the common nomenclature used in the literature, being g the energy distribution function. In this paper, the collision operator is modeled considering a single relaxation time according to Bhatnagar *et al.* (1954), given by: $\Omega = \frac{1}{\tau} \cdot (g^{eq} - g)$. In this relation, g^{eq} represents the equilibrium distribution function, which is related with the particles in equilibrium state and can be calculated by: $g^{eq}(\mathbf{x}, t) = w_i \cdot T(\mathbf{x}, t)$ (see Krüger *et al.* (2017)). w_i represents the weights related with the velocity scheme chosen. In this paper, it is used the D2Q9 scheme, meaning that for a 2D simulation there are 9 discrete velocity directions. Thus, for this scheme, the weights are $w_0 = 4/9$, $w_{1,2,3,4} = 1/9$ and $w_{5,6,7,8} = 1/9$ (Guo and Shu, 2013). The paramenter τ is the single relaxation time, which is related to fluid (or solid) thermal properties as shown in Eq. (2).

$$\tau = \frac{\alpha \cdot \Delta t}{c_s^2 \cdot \Delta x^2} + 0.5 \tag{2}$$

In this equation, α is the thermal diffusivity of the material, Δx and Δt are the space and time discretization intervals and c_s is the sound speed, in lattice units (for D2Q9, it is assumed $c_s = 1/\sqrt{3}$). Using the defined variables and after discretizing the Boltzmann equation (Eq. (1)), the final expression for thermal LBM resides in Eq. (3), in which the sub-index i indicates each velocity direction.

$$g_i(\mathbf{x} + \mathbf{c_i} \cdot \Delta t, t + \Delta t) = g_i(\mathbf{x}, t) + \frac{1}{\tau} \cdot [g_i^{eq}(\mathbf{x}, t) - g_i(\mathbf{x}, t)] \tag{3}$$

Additionally, the distribution function is related with macroscopic quantities (such as the temperature T) by its moments: $\int g(\mathbf{x}, t) dc = T(\mathbf{x}, t)$. So, after solving Eq. (3), it is possible to calculate the temperature field using the Eq. (4), being q the total number of discrete velocity directions.

$$\sum_{i=0}^{q-1} g_i(\mathbf{x}, t) = T(\mathbf{x}, t) \tag{4}$$

Employing the above relations, it becomes possible to apply the LBM and get the desired values for each situation analyzed. For that, a computational procedure is implemented, which can be divided in four principal steps: initialization, collision, streaming with boundary conditions and calculation of macroscopic variables. The three last are repeated until the desired time steps are gotten or the steady state condition is satisfied.

Nevertheless, it is important to note that, for the initialization step, a good approach is to assume that the distribution functions g_i are in equilibrium. In other words, it is possible to initialize these functions as $g_i = g_i^{eq}$ (Krüger *et al.*, 2017) (Guo and Shu, 2013). Another important point to be noted is that the condition chosen to verify the steady state has a great influence on the final results, mainly when the problem studied involves materials with low thermal diffusivities. Thus, for the problems analyzed in this work, the scheme used to verify this state is given by Eq. (5) , in which n represents the current time step and $n - 1000$, 1000 time steps before n.

$$e = max|T^n - T^{n-1000}| \leq 10^{-6} \tag{5}$$

Moreover, there are two principal formulations of the collision operator: the BGK model and the multiple-relaxation-time (MRT) operator. The first (BGK) is based in the approach showed before, resulting in Eq. (6), in which g_i^* are the post-collision distribution function, which are streamed after collision step accordingly each velocity direction: $g_i(\mathbf{x} + \mathbf{c_i} \cdot \Delta t, t + \Delta t) = g_i^*(\mathbf{x}, t)$. However, as the simplicity of the BGK operator comes with some reduced accuracy, there are some situations in which it is necessary to increase the precision of the results. These cases demand the use of more accurate collision operator, such as the MRT, which will be discussed bellow.

$$g_i^*(\mathbf{x}, t) = g_i(\mathbf{x}, t) + \frac{1}{\tau} \cdot [g_i^{eq}(\mathbf{x}, t) - g_i(\mathbf{x}, t)] \tag{6}$$

2.1 MRT collision operator

The main idea behind the MRT collision operator is first map the distribution function in moment space, then compute the collision step, to finally transfer these collided moments to the distribution function. Then, defining $m_i(\mathbf{x},t)$ as the moment of each velocity direction i, $m_i^{eq}(\mathbf{x},t)$ as their respective equilibrium distribution function and $m_i^*(\mathbf{x},t)$, the post-collision moments, the collision step is given by Eq. (7).

$$\{m^*(\mathbf{x},t)\} = \{m(\mathbf{x},t)\} - [S]\left(\{m(\mathbf{x},t)\} - \{m^{eq}(\mathbf{x},t)\}\right) \tag{7}$$

In Eq. (7), the moments are represented by a vector with the moments in each velocity direction, and $[S]$ are a diagonal matrix with the multiple relaxation parameters. Thus, accordingly to Chai and Zhao (2014), for the D2Q9 scheme in thermal LBM, a reasonable choice of this matrix is $[S] = diag(0.0, 1.0, 1.0, \omega, 1.0, \omega, 1.0, 1.0, 1.0)$, being $\omega = 1/\tau$.

Furthermore, in order to transfer the values of $g_i(\mathbf{x},t)$ to moment space it is defined a transform matrix $[M]$ so that $\{m(\mathbf{x},t)\} = [M]\cdot\{g(\mathbf{x},t)\}$. Then, following the same procedure proposed by Guo and Shu (2013), this matrix can be given by Eq. (8). The equilibrium moments can be obtained by the same way as the moments are gotten, calculating first the values of $g_i^{eq}(\mathbf{x},t)$, and then applying the equation $\{m^{eq}(\mathbf{x},t)\} = [M]\cdot\{g^{eq(\mathbf{x},t)}\}$.

$$[M] = \begin{bmatrix} 1 & 1 & 1 & 1 & 1 & 1 & 1 & 1 & 1 \\ -4 & -1 & -1 & -1 & 2 & 2 & 2 & 2 & 2 \\ 4 & -2 & -2 & -2 & -2 & 1 & 1 & 1 & 1 \\ 0 & 1 & 0 & -1 & 0 & 1 & -1 & -1 & 1 \\ 0 & -2 & 0 & -2 & 0 & 1 & -1 & -1 & 1 \\ 0 & 0 & 1 & 0 & -1 & 1 & 1 & -1 & -1 \\ 0 & 0 & -2 & 0 & -2 & 1 & 1 & -1 & -1 \\ 0 & 1 & -1 & 1 & -1 & 0 & 0 & 0 & 0 \\ 0 & 0 & 0 & 0 & 0 & 1 & -1 & 1 & -1 \end{bmatrix} \tag{8}$$

After calculating the collision step, the post-collision functions can be extracted of the moment space doing the inverse of the procedure explained before: $\{g(\mathbf{x},t)\} = [M]^{-1}\cdot\{m(\mathbf{x},t)\}$, being $[M]^{-1}$ the inverse of the transform matrix. By this relationship, in general, the collision step can be calculated by Eq. (9).

$$\{g^*(\mathbf{x},t)\} = [M]^{-1}\cdot\left(\{m(\mathbf{x},t)\} - [S]\left(\{m(\mathbf{x},t)\} - \{m^{eq}(\mathbf{x},t)\}\right)\right) \tag{9}$$

2.2 Boundary conditions

For the problems studied in this work, it was considered both Neumann and Dirichlet boundary conditions. In this way, it is important to guarantee that these conditions are properly calculated.

First, considering a Dirichlet boundary condition in which the temperature of the wall T_w is known, the procedure given by Yoshino and Inamuro (2003) is followed. In this work, it is assumed that the unknown populations are in equilibrium with some unknown temperature T'. Then, by the conservation of mass (Eq. (4)), it is possible to define the Eq. (10), where $\mathbf{n}$ is the normal vector of each boundary label, pointing to the interior of the domain. So, the population desired can be obtained by $g_i = g_i^{eq}(T')$.

$$T' = \frac{T_w - \sum\limits_{\mathbf{c}\cdot\mathbf{n}\leq 0} g_i}{\sum\limits_{\mathbf{c}\cdot\mathbf{n}>0} w_i} \tag{10}$$

The next condition to be treated is the Neumann boundary condition, which is referred to the known heat flux at the domain boundaries. In this case, it was applied a numerical discretization of Fourier's Law in order to transform this condition into a Dirichlet's boundary condition. In this way, it was used the finite difference method, that gives the relation shown by Eq. (11)(Zhang and Cheng, 2017), where T_{w+1} is the temperature of the node after the boundary node in the normal direction, q'' is the heat flux and k, the conductivity of the material, in W/(m.K). Thus, knowing T_w it is possible to apply the Inamuro's method for Dirichlet boundary condition.

$$T_w = T_{w+1} + \frac{q''|\mathbf{x_w} - \mathbf{x_{w+1}}|}{k} \tag{11}$$

However, it is important to say that, for adiabatic walls, it was used a different method: the Bounce-Back rule. Despite of being first developed for walls in fluid flow problems, the same principle of this rule can be applied to insulated walls, because the heat flux crossing these boundaries is zero, which means that there are none particles crossing these boundary lines. In other words, the particles which hit in the boundary are totally reflected in opposite direction (are bounced back) (Ho *et al.*, 2002). If $\bar{i}$ is the opposite direction of i, this method can be represented by: $g_i = g_{\bar{i}}$.

2.3 Interface conditions

In situations that involves two or more materials, it is important to guarantee the continuity of the physical quantities despite of the non-continuity of the thermal properties at interface. In this way, at each interface between different domains, it must be kept the same temperature and heat flux.

Considering two materials such as in the Fig. 4, defining the thermal properties ratio such as $\gamma = \frac{(\rho \cdot Cp)_{sb}}{(\rho \cdot Cp)_{st}}$ and following the boundary conditions proposed by Li *et al.* (2014), it is possible to define some relationships between the populations that cross the interface. Then, to keep the temperature and the heat flux continuous at this line, it is necessary to apply the Eq. (12) to the populations arriving in the upper material (index st), after leaving the bottom one, and Eq. (13) to the populations arriving in the bottom (index sb), after leaving the upper material.

$$g_{\bar{i}}(\mathbf{x_{st}}, t + \Delta t) = \frac{1-\gamma}{1+\gamma} \cdot g_i^*(\mathbf{x_{st}}, t) + \frac{2\gamma}{1+\gamma} \cdot g_{\bar{i}}^*(\mathbf{x_{sb}}, t) \tag{12}$$

$$g_i(\mathbf{x_{sb}}, t + \Delta t) = -\frac{1-\gamma}{1+\gamma} \cdot g_{\bar{i}}^*(\mathbf{x_{sb}}, t) + \frac{2}{1+\gamma} \cdot g_i^*(\mathbf{x_{st}}, t) \tag{13}$$

2.4 Multi-block scheme

The conventional LBM uses an uniform discretization of the domain in equal lattices. On the other hand, the Multi-block scheme allows to divide the domain in several parts, each one with some different size of lattices. It is important to note that some attention must be given to the transport of information between the different grids. Also, the division in different grids comes whit different time steps for each one, that must be respected in the transport of information in the grid interfaces.

In order to discuss this method and propose its improvement, it was first followed the procedure presented by Zhang *et al.* (2019) and Yu *et al.* (2002). Considering first only 2 different grids, it is defined the ratio between them as $m = \Delta x_c / \Delta x_f$, in which the sub-index f is related with the fine grid and c, with the coarse grid. Then, it is necessary to maintain the continuity of the thermal properties between the different regions, giving $\tau_f = 0,5 + m \cdot (\tau_c - 0,5)$ (Liu *et al.*, 2009). Because of that relation, the choice of the time steps sizes Δt_f and Δt_c is not free. Thus, there is some proportion that must be kept between the time and spatial discretization, when this relation is allocated together with the Eq. (2), which gives that $\Delta t_c / \Delta t_f = m$.

Moreover, there are two principal lines whoch demarcate the end of each grid in the interfaces for 2D simulations. It is important to note that these lines are not coincident, in order of having some lattices which just receive the information becoming of the other grid, after streaming them into their part of domain. The representation of the both interface between two different grids can be seen in Fig. 1, in which MN represents the interface of the fine grid (where it receives information from the coarse grid) and AB, the coarse grid interface (where it receives information from the fine grid).

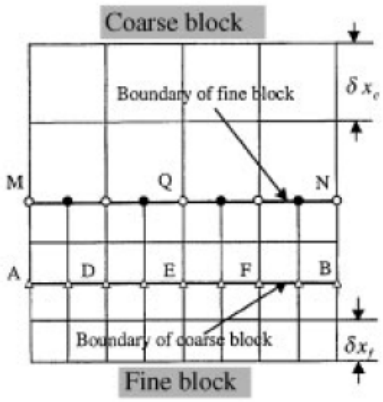

Figure 1. Illustration of some domain whit two different grids of lattices and its interfaces (Yu *et al.*, 2002).

Thereby, it is necessary to keep the continuity of the physical quantities at these interfaces during the transport of information between them. First, considering the continuity of the temperature field, it gives: $g_{c,i}^{eq} = g_{f,i}^{eq}$. Second, the same must be done for the heat flux. Defining it as $\mathbf{J} = (1 - \frac{1}{2\tau}) \sum_i g_i^{neq} \mathbf{c_i}$ (Chai and Zhao, 2013), in which g_i^{neq} are the non-equilibrium distribution functions ($g_i^{neq} = g_i - g_i^{eq}$), it is possible to get $\left(1 - \frac{1}{2\tau_c}\right) g_{c,i}^{neq} = \left(1 - \frac{1}{2\tau_f}\right) g_{f,i}^{neq}$. With these two relations, it is possible to find how the information between the interfaces are carried, which is represented by Eq. (14) and Eq. (15). As it is possible to note, because of the different time and space discretization, each grid has its own relaxation parameter.

$$g_{c,i}^{*} = g_{f,i}^{eq} + m\frac{\tau_c - 1}{\tau_f - 1}(g_{f,i}^{*} - g_{f,i}^{eq}) \tag{14}$$

$$g_{f,i}^{*} = g_{c,i}^{eq} + \frac{\tau_f - 1}{m(\tau_c - 1)}(g_{c,i}^{*} - g_{c,i}^{eq}) \tag{15}$$

However, as it is possible to see in Fig. 1, the nodes of the coarse grid does not match with all nodes of fine grid. Thus, it is necessary to do a spatial interpolation in order to get the values of the functions coming from coarse grid on • nodes. For this, it is used an spline cubic interpolation such as in Eq. (16), in which $g_i(x)$ could represents even $g_{c,i}^{*}$ or $g_{c,i}^{eq}$, being x the direction of the interface (such as the direction of the line MN in Fig. 1).

$$g_i(x) = a_j(x_j - x)^3 + b_j(x - x_{j-1})^3 + c_j(x_j - x) + d_j(x - x_{j-1}) \tag{16}$$

Thereby, according to Zhang *et al.* (2019), the constants in Eq. (16) can be defined as $a_j = \frac{g''_{j-1}}{6h_j}$, $b_j = \frac{g''_j}{6h_j}$, $c_j = \frac{g_{j-1}}{h_j} - \frac{g''_{j-1}h_j}{6}$, $d_j = \frac{g_j}{h_j} - \frac{g''_j h_j}{6}$, where g''_j is the second derivative of f^* or f^{eq} in j position over the interface line and $h_j = x_j - x_{j-1}$. Additionally, to find the values of g''_j, it is possible to solve an simple three diagonal linear system given by $0,5g''_{j-1} + 2g''_j + 0,5g''_{j+1} = 6g_j - 3g_{j-1} - 3g_{j+1}$, considering that $g''_0 = g''_N = 0$.

Also, there are time steps for which the fine grid will need values of the coarse grid in an interval in which it will not be part of. For these steps, it is necessary to do some temporal interpolation in order to get these needed values. In this case, it was chosen a 3 points Lagrangian interpolation of $g_{c,i}^{*}$ or $g_{c,i}^{eq}$ in steps $n-1$, n and $n+1$ of the coarse grid. This procedure can be represented by Eq. (17), with $t_n < t < t_{n+1}$.

$$f_i^{*f}(t) = \sum_{k=n-1}^{n+1} f_i^{*f}(t_k) \left(\prod_{j=n-1; j\neq k}^{n+1} \frac{t - t_j}{t_k - t_j} \right) \tag{17}$$

2.5 Improved Multi-block scheme

Following the same procedure as Yu *et al.* (2002), but now defining a time ratio as $m_t = \Delta t_c / \Delta t_f$, to guarantee the continuity of the thermal diffusivity: $\alpha_f = \alpha_c$. Then, by Eq. (2), the new relation to be kept is $\tau_f = 0,5 + (m^2/m_t)(\tau_c - 0,5)$. Thus, the final relation to transfer the functions between the different grids can be given by Eq. (18) and Eq. (19).

$$g_{c,i}^{*} = g_{f,i}^{eq} + \frac{m^2}{m_t}\frac{(\tau_c - 1)}{(\tau_f - 1)}(g_{f,i}^{*} - g_{f,i}^{eq}) \tag{18}$$

$$g_{f,i}^{*} = g_{c,i}^{eq} + \frac{m_t}{m^2}\frac{(\tau_f - 1)}{(\tau_c - 1)}(g_{c,i}^{*} - g_{c,i}^{eq}) \tag{19}$$

Then, with this improvement of the multi-block scheme, it is possible to flexibilize much more the method, which is extremely important when it is necessary to adjust high values of relaxation time. This because its allows get lowers τ values then with the conventional MB-LBM, as in this method it is necessary to guarantee that $m_t = m$. For example, in conjugate heat transfer problems generally there are materials with high difference between their thermal diffusivity and, consequently, between their τ, which can impact in the accuracy of the simulations, even if it is used the MRT collision operator.

3. Results and discussion

3.1 Two-dimensional conduction in a single material

First, in order to verify the implementation of the Multi-block scheme with the conventional LBM, a simple 2D conduction problem was solved. The domain was divided into two grids, such as in Fig. 2(b), in which the coarse grid is about 4x the fine grid. The results were compared with the obtained analytical solution represented by Eq. (21), where q'' is the heat flux of 10000 W/m^2 and T_W, the wall temperature about 293.15K. The boundary conditions considered can be seen in Eq. (20). Also, λ_n is defined as $\lambda_n = \frac{(1+2n)\pi}{2a}$, being the domain width a = 0.5 m and height b = 0.3 m, respectively.

$$\begin{cases} T(x,y) = T_w, & \text{for } x = 0; \\ \frac{\partial T}{\partial x} = 0, & \text{for } x = a; \\ \frac{\partial T}{\partial y} = 0, & \text{for } y = 0; \\ q'' = k\frac{\partial T}{\partial y}, & \text{for } y = b; \end{cases} \tag{20}$$

$$T(x,y) = T_w + \sum_{n=0}^{\infty} \frac{2 \cdot q'' \cdot sin(\lambda_n \cdot x) \cdot cosh(\lambda_n \cdot y)}{k \cdot \lambda_n^2 \cdot sinh(\lambda_n \cdot b) \cdot a} \tag{21}$$

It was verified an average absolute error equal to 0.1139 K, which is considered satisfactory. It was also simulated the same problem with the conventional LBM, using the same grid as the fine grid used in previous simulation, finding an average absolute error of 0.1162 K, verifying the employ MB-LBM in the solved conduction heat transfer problem.

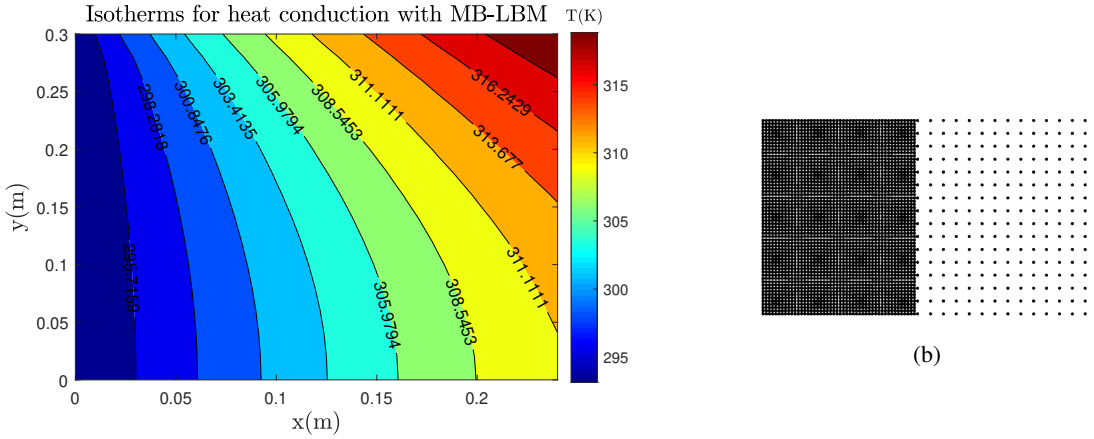

Figure 2. In (a): Results given by the MB-LBM for the heat conduction, using a fine grid with Δx = 0.005 m and Δt = 0.02 s, and a coarser grid of Δx = 0.02 m and Δt = 0.08 s. In (b): representation of the used grid.

3.2 One-dimensional conduction between two solids

Therefore, the next study proposed was the conduction between two solids, in order to analyze the impact of having two materials with high difference between their thermal diffusivities (α). For that, first it was proposed a one-dimensional problem involving two solids with similar α, in which the boundary conditions consists in a constant heat flux q'' = 1000 W/m^2 for $x = 0$ m and a constant temperature $T_w = 293.15$K, for $x = 0.5$ m. The analytical solution and the boundary conditions are showed in Eq. (22), being x_2 the domain width (about 0.5 m) and x_1, the interface at 0.25 m. Moreover, it was defined that the domain is copper for 0 m $\leq x \leq$ 0.25 m and silicon for 0.25 m $< x \leq$ 0.5, being k_{Si} and k_{Cu} the thermal conductivity of the silicon and copper, respectively.

$$\begin{cases} q'' = -k_{Cu}\frac{dT}{dx}, & \text{for } x = 0; \\ T(x) = T_w, & \text{for } x = x_2; \\ T(x) = T_w + q'' \cdot \left[\frac{(x_1 - x)}{k_{Cu}} + \frac{(x_2 - x_1)}{k_{Si}}\right], & \text{if } 0 < x \leq x_1; \\ T(x) = T_w + q'' \cdot \left[\frac{(x_2 - x)}{k_{Si}}\right], & \text{if } x_1 \leq x < x_2; \end{cases} \tag{22}$$

Using the conventional LBM it was found an absolute average error equal to 0.0259 K in relation to the analytical solution. Almost the same error was found using the MB-LBM method, and by this reason these results are not shown in the paper. The results given by the conventional LBM and the analytical solution can be seen in Fig. 3

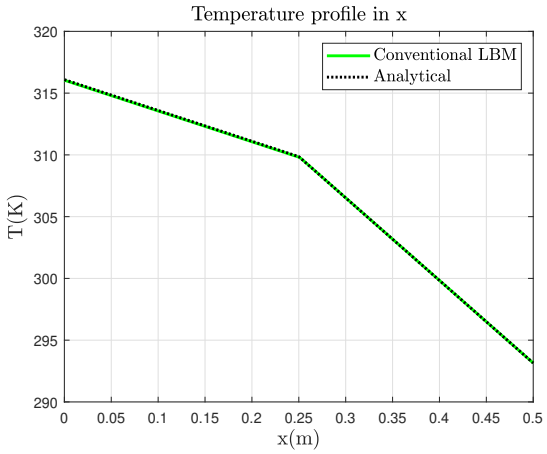

Figure 3. Comparison between the temperature profile in x direction given by the conventional LBM and by the analytical solution.

In problems such as the previous one, there are not a large difference between the thermal properties of the materials, and the conventional LBM is enough. However, difficulties appear when it is selected materials with large difference between theirs α, for example water and silicon. This is mainly because of the difficulty in obtaining good values for each relaxation time. This fact impacts in the accuracy of the method, because the error of the simulation results increases as τ values become high than unity (Krüger *et al.*, 2017). Because of that, it is proposed the improved MB-LBM.

3.3 Two-dimensional conduction between two solids

The commented difficulties are tested considering the solution of the problem exposed in Fig. 4, using an hypothetical solid material with the same thermal properties of water. This was done in order to resemble a problem of a conjugate heat transfer in a channel, commonly found in refrigerating systems, but avoiding any loss of precision coming from the simulation of fluid flow. This allows to isolate the issue of losing accuracy because of high values of τ.

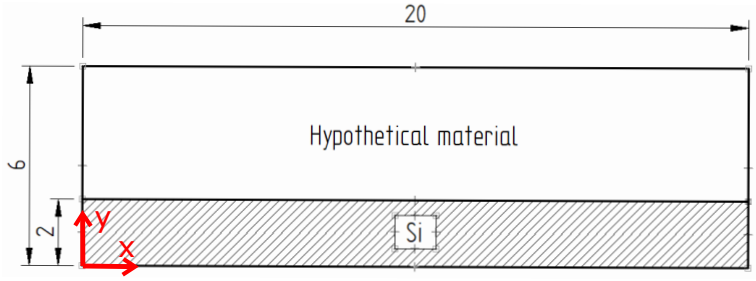

Figure 4. Scheme with dimensions (in mm) for the heat diffusion problem involving two solids with large difference between their α.

$$\begin{cases} T(x,y) = T_w, & \text{for } x = 0\text{m}; \\ \frac{\partial T}{\partial x} = 0, & \text{for } x = 0.02\text{m}; \\ q'' = -k_{Si}\frac{\partial T}{\partial y}, & \text{for } y = 0\text{m}; \\ \frac{\partial T}{\partial y} = 0, & \text{for } y = 0.006\text{m}; \end{cases} \tag{23}$$

Hence, the problem was treated both with conventional LBM and improved MB-LBM, both using the MRT collision operator. The obtained results were compared with the solution given by the software COMSOL, in order to verify the errors for each method. For the MB-LBM, it was chosen one grid for each material, keeping the coarse grid in the bottom solid (because of a coarse grid reduces more the value of τ, with correct values of Δt_c). It was also studied the effects of the grid refinement in the conventional LBM (Fig. 7), as the impact of increasing the relaxation parameter with the MB-LBM and the improved MB-LBM (Fig. 8). The solution for each method can be seen in Fig. 5 and Fig. 6.

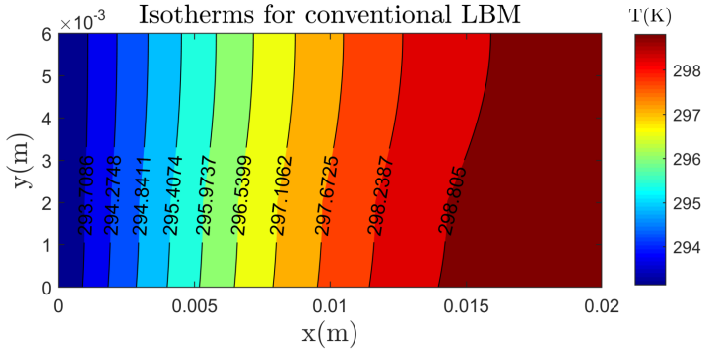

(a)

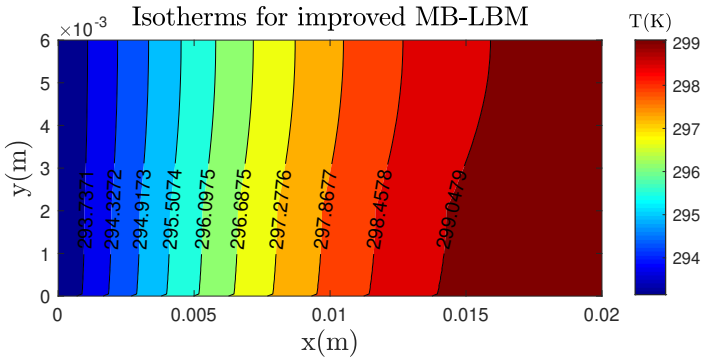

(b)

Figure 5. Isotherms for the conventional LBM (a), with $\Delta x = 5.0 \cdot 10^{-5}$ m and $\Delta t = 1.25 \cdot 10^{-4}$ s, and for the improved MB-LBM (b), with a coarser grid of $\Delta x_c = 2.0 \cdot 10^{-4}$ m and $\Delta t_c = 3.75 \cdot 10^{-4}$ s and a fine grid of $\Delta x_f = 0.5 \cdot 10^{-4}$ m and $\Delta t_f = 1.25 \cdot 10^{-4}$ s.

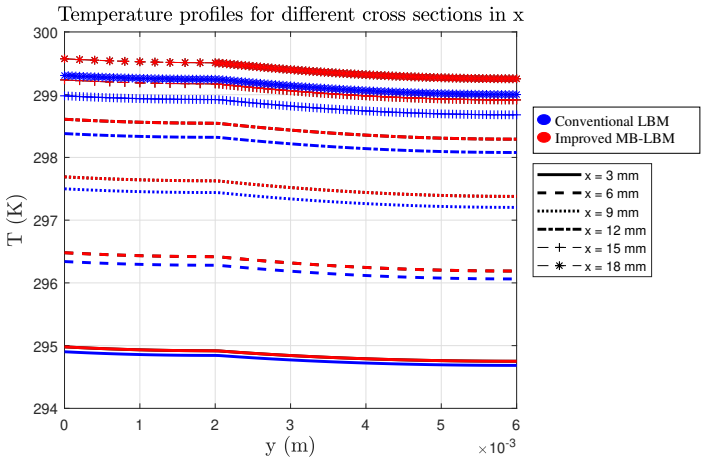

Figure 6. Temperature profiles for different cross sections in x for both conventional LBM (blue), with $\Delta x = 5.0 \cdot 10^{-5}$ m and $\Delta t = 1.25 \cdot 10^{-4}$ s, and improved MB-LBM (red), with a coarser grid of $\Delta x_c = 2.0 \cdot 10^{-4}$ m and $\Delta t_c = 3.75 \cdot 10^{-4}$ s and a fine grid of $\Delta x_f = 0.5 \cdot 10^{-4}$ m and $\Delta t_f = 1.25 \cdot 10^{-4}$ s.

Beforehand, it is possible to note the increase of the LBM accuracy with the grid refinement, as the average absolute error reduces progressively in Fig. 7. However, even reducing the size of the mesh more than that for the MB-LBM, the errors of LBM are still higher. This fact can be explained by the high values of the relaxation parameter for the bottom solid, because the values of both τ must not be too closer of 0.5 (Krüger *et al.*, 2017), and to satisfy this condition in the upper solid, the values of this parameter becomes much high than unity for the bottom solid.

In these simulations, the lowest τ value gotten to still guarantee the stability of the method was 0.52 for upper material and 14.08 for bottom material. However, for improved MB-LBM, these values were 0.52 and 3.05, respectively, and for the conventional MB-LBM, 0.52 and 2.20. This fact explain why the both MB-LBM shows a greater precision even using an coarse grid than the conventional LBM, as it is possible to see when both Fig. 7 and Fig. 8 are compared. Moreover, the effect of increasing τ becomes clearer in Fig. 8, in which it was kept the same mesh for the improved MB-LBM, just

varying the values of the relaxation time, increasing the average absolute error.

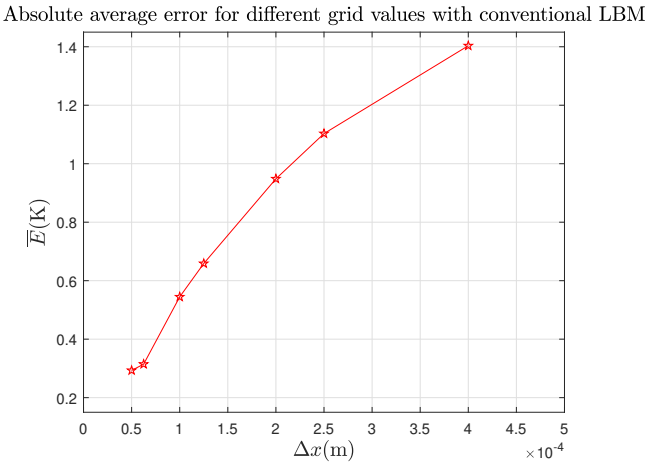

Figure 7. Error evolution with mesh refinement for conventional LBM.

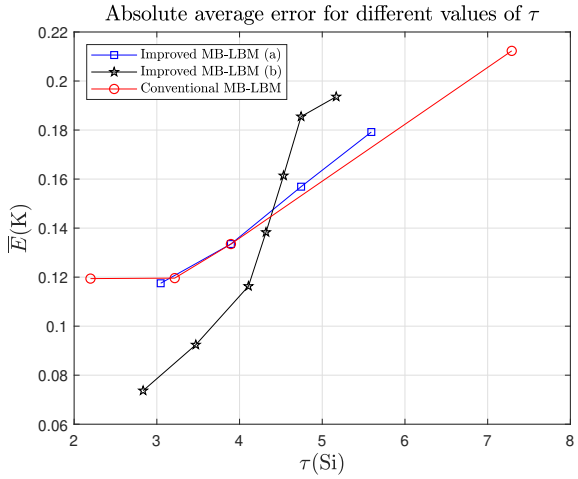

Figure 8. Error evolution with relaxation time increasing for conventional MB-LBM, with $\Delta x_f = 0.5 \cdot 10^{-4}$m fix and $\Delta x_c = 2.0, 2.5, 4.0 \cdot 10^{-4}$m for $\tau = 2.2, 3.2, 3.9, 7.3$, respectively; and improved MB-LBM, for fix values of Δx_f and Δx_c, being (a):$\Delta x_f = 0.5 \cdot 10^{-4}$m and $\Delta x_c = 2.0 \cdot 10^{-4}$m, (b): $\Delta x_f = 0.5 \cdot 10^{-4}$m and $\Delta x_c = 4.0 \cdot 10^{-4}$m.

Furthermore, it is important to say that, with the conventional MB scheme, it would be not possible to reduce the effects of relaxation parameter in the method precision such as it was reduced with the improved MB, due to the Δt dependence of Δx. This is because, when the conventional MB-LBM starts to become more precise in relation to τ values, the coarse grid has to be poorly refined, stopping or even reducing the accuracy of the method. This occurs because, to reducing τ, it is necessary to increase both Δt_c and Δx_c in order to keep the relation $m = m_t$. So, the main advantage of improved MB-LBM is that it does not need to satisfy this relationship, allowing to change the m without changing m_t. This means that the improved MB-LBM has an additional degree of freedom to choose the τ values.

This fact can be seen in Fig. 8, in which it is shown the possibility of using several τ values for a fixed mesh dimension when using the improved MB-LBM. In this figure, it is important to effort that to change the values of τ in conventional MB-LBM, it was not possible to keep the same grid for all simulations because of $m = m_t$, differently for the improved MB-LBM. Despite of both methods showing almost the same errors, it is noted that the conventional MB-LBM does not allow to change the Δt_c independently of Δx_c, after some relaxation time value ($\tau = 3.2$). Thus, the new approach proposed for MB-LBM increase the application range of this method as its accuracy, by allowing the correct adjustment of τ in each part of the domain. In the present problem, a better accuracy was obtained for the improved MB-LBM using fix $\Delta x_f = 0.5 \cdot 10^{-4}$m and $\Delta x_c = 4.0 \cdot 10^{-4}$m.

4. Conclusion

In general, it was possible to develop, test and verify an improvement of the Multi-block scheme applied to the LBM, solving 2D heat conduction problems. It was showed how the high values of relaxation time (τ) and large differences between the thermal diffusivity of the materials allied with the convergence limits of τ would decrease the conventional

LBM accuracy. Thus, the method can find difficulties in treating several real conjugate heat transfer problems, because most of these problems include high α solids with low α fluids. These effects can be perceived when it is compared the situation in Fig. 3, where the values of α of both solids are closer, and in Fig. 5, where there is a large difference between their thermal diffusivities.

So, in order to solve this issue, it was proposed the improved MB-LBM, discretizing each material of the domain with a mesh that reaches good values for each relaxation time, accordingly with each thermal diffusivity. It is important to see that it is also possible to adjust τ with the conventional MB-LBM, but because of the dependence between the time and space discretization ratios ($m = m_t$), it is not possible to get such τ good values in some situations as with the improved MB-LBM. This is because when the conventional MB-LBM starts to become more precise in relation to τ values, the coarse grid has to be poorly refined, decreasing the precision of the results, as showed by Fig. 8.

Also, it was obtained very satisfactory simulation results with the proposed MB-LBM, as it is possible to note in Fig. 6. Thus, the same procedure can be applied in conjugate heat transfer problems that involves fluid flow, with the intention of increasing the accuracy of the results adopting one specific grid for each part of domain, choosing the correct values of Δx and Δt that should allow to obtain good values of τ.

5. ACKNOWLEDGMENTS

The authors are grateful for the financial assistance granted by the São Paulo State Research Foundation (FAPESP), processes 2019/21022-9 and 2016/09509-1; and by the National Council for Scientific and Technological Development (CNPq), process 431782/2018-0.

6. REFERENCES

Aursjø, Jettestuen, E., Vinningland, J.L. and Hiorth, A., 2017. "An improved lattice boltzmann method for simulating advective-diffusive processes in fluids". *Journal of Computational Physics*, Vol. 332, No. 8, pp. 363–375.

Bhatnagar, P.L., Gross, E.P. and Krook, M., 1954. "A model for collision processes in gases i: Small amplitude processes in charged and neutral one-component systems". *Physical Review*, Vol. 94, pp. 511–525.

Chai, Z. and Zhao, T.S., 2013. "Lattice boltzmann model for the convection-diffusion equation". *Physical Review*, Vol. 87, p. 063309.

Chai, Z. and Zhao, T.S., 2014. "Nonequilibrium scheme for computing the flux of the convection-diffusion equation in the framework of the lattice boltzmann method". *Physical Review E*, Vol. 90, p. 013305.

Guo, Z. and Shu, C., 2013. *Lattice Boltzmann Method and its Application in Angineering*. World Scientific Publishing Co. Pte. Ltd., Singapore.

Ho, J.R., Kuo, C.P., Jiaung, W.S. and Twu, C., 2002. "Lattice boltzmann scheme for hyperbolic heat conduction equation". *Numer. Heat Transfer, Part B:Fundamentals: An Int. J. of Comp. and Method.*, Vol. 41:6, pp. 591–607.

Krüger, T., Kusumaatmaja, H., Shardt, A.K.O., Silva, G. and Viggen, E.M., 2017. *Lattice Boltzmann Method: Principles and Practice, 2nd Edition*. Springer International Publishing AG, Cham.

Li, L., Mei, R. and Klausner, J.F., 2014. "Conjugate heat and mass transfer in the lattice boltzmann equation method". *Physical review E*, Vol. 89, p. 043308.

Liu, H., Zhou, J.G. and Burrows, R., 2009. "Multi-block lattice boltzmann simulations of subcritical flow in open channel junctions". *Computers & Fluids*, Vol. 36, p. 1108–1117.

Mohamad, A.A., 2019. *Lattice Boltzmann Method - Fundamentals and Engineering Applications*. Springer-Verlag London Ltd., part of Springer Nature.

Pirouz, M.M., Farhadi, M., Sedighi, K., Nemati, H. and Fattahi, E., 2011. "Lattice boltzmann simulation of conjugate heat transfer in a rectangular channel with wall-mounted obstacles". *Scientia Iranica B*, Vol. 18, No. 2, p. 213–221.

Wang, J., Wang, M. and Li, Z., 2007. "A lattice boltzmann algorithm for fluid–solid conjugate heat transfer". *International Journal of Thermal Sciences*, Vol. 46, p. 228–234.

Wolf-Gladrow, D.A., 2004. *Lattice-gas cellular automata and lattice Boltzmann models: an introduction*. Springer.

Yoshino, M. and Inamuro, T., 2003. "Lattice boltzmann simulations for flow and heat/mass transfer problems in a three-dimensional porous structure". *International Journal of Numerical Methods in Fluids*, Vol. 43, p. 183–198.

Yu, D., Mei, R. and Shyy, W., 2002. "A multi-block lattice boltzmann method for viscous fluid flows". *International Journal for Numerical Method in Fluids*, Vol. 39, pp. 99–120.

Zhang, C. and Cheng, P., 2017. "Mesoscale simulations of boiling curves and boiling hysteresis under constant wall temperature and constant heat flux conditions". *International Journal of Heat and Mass Transfer*, Vol. 110, p. 319–329.

Zhang, Y., Pan, G. and Huang, Q., 2019. "The implementation of multi-block lattice boltzmann method on gpu". *International Journal of Computational Methods*, Vol. 16, No. 5, p. 1840002.

7. RESPONSIBILITY NOTICE

The authors are solely responsible for the printed material included in this paper.